Peptides 81 (2016) 29–37

Contents lists available at ScienceDirect

Peptides

journal homepage: www.elsevier.com/locate/peptides

Adropin reduces paracellular permeability of rat brain endothelial cells exposed to ischemia-like conditions

Changjun Yang, Kelly M. DeMars, Kimberly E. Hawkins, Eduardo Candelario-Jalil*

Department of Neuroscience, McKnight Brain Institute, University of Florida, Gainesville, FL 32610, USA

ARTICLE INFO

Article history:
Received 17 December 2015
Received in revised form 1 March 2016
Accepted 23 March 2016
Available online 25 March 2016

Keywords:
Adropin
Hypoxia
Paracellular permeability
Tight junction proteins
Adherens junction protein
Myosin light chain 2
Rho-associated kinase

ABSTRACT

Adropin is a peptide encoded by the energy homeostasis associated gene (*Enho*) and plays a critical role in the regulation of lipid metabolism, insulin sensitivity, and endothelial function. Little is known of the effects of adropin in the brain and whether this peptide modulates ischemia-induced blood-brain barrier (BBB) injury. Here, we used an *in vitro* BBB model of rat brain microvascular endothelial cells (RBE4) and hypothesized that adropin would reduce endothelial permeability during ischemic conditions. To mimic ischemic conditions *in vitro*, RBE4 cell monolayers were subjected to 16 h hypoxia/low glucose (HLG). This resulted in a significant increase in paracellular permeability to FITC-labeled dextran (40 kDa), a dramatic upregulation of vascular endothelial growth factor (VEGF), and the loss of junction proteins occludin and VE-cadherin. Notably, HLG also significantly decreased *Enho* expression and adropin levels. Treatment of RBE4 cells with synthetic adropin (1, 10 and 100 ng/ml) concentration-dependently reduced endothelial permeability after HLG, but this was not mediated through protection to junction proteins or through reduced levels of VEGF. We found that HLG dramatically increased myosin light chain 2 (MLC2) phosphorylation in RBE4 cells, which was significantly reduced by adropin treatment. We also found that HLG significantly increased Rho-associated kinase (ROCK) activity, a critical upstream effector of MLC2 phosphorylation, and that adropin treatment attenuated that effect. These data indicate that treatment with adropin reduces endothelial cell permeability after HLG insult by inhibition of the ROCK-MLC2 signaling pathway. These promising findings suggest that adropin protects against endothelial barrier dysfunction during ischemic conditions.

1. Introduction

Ischemic stroke is a leading cause of death and permanent disability worldwide. Opening of the blood-brain barrier (BBB) correlates with increased edema, hemorrhagic transformation, and ultimately worse outcome in ischemic stroke patients [12,25,41]. One of the main components of the BBB is the endothelial cell monolayer, held tightly together by tight junctions and adherens junctions. Reducing BBB breakdown by protecting the endothelium is a critical target for potential stroke therapeutics.

Adropin is a highly conserved polypeptide containing a secretory signal peptide encoded by N-terminal amino acid residues 1–33, and a putative secreted domain, adropin$^{34-76}$ [24]. This polypeptide is abundantly expressed in the liver and brain of many mammals including humans, and is encoded by the energy homeostasis associated gene (*Enho*) [24,42]. Previously, adropin has been shown to be an important regulator of adiposity, insulin resistance, and glucose tolerance [17,18,24,42]. Recent studies found that low plasma adropin levels were closely associated with endothelial dysfunction in patients with diabetes or cardiovascular diseases [10,20,39,43,46]. Also, an *in vitro* study found that adropin-treated human umbilical vein and coronary artery endothelial cells exhibited reduced endothelial monolayer permeability and greater cell proliferation and migration mediated through the vascular endothelial growth factor receptor-2

Abbreviations: BBB, blood-brain barrier; RBE4, rat brain microvascular endothelial cells; HLG, hypoxia/low glucose; FITC-dextran, fluorescein isothiocyanate–dextran; HIF-1α, hypoxia inducible factor-1alpha; VEGF, vascular endothelial growth factor; TJ, tight junction; AJ, adherens junction; ZO-1, zonula occludens-1; VE-cadherin, vascular endothelial cadherin; ELISA, enzyme-linked immunosorbent assay; MLC2, myosin light chain 2; ROCK, Rho-associated kinase; MLCP, myosin light chain phosphatase; MLCK, myosin light chain kinase; *Enho*, energy homeostasis associated gene; Akt, protein kinase B; ERK1/2, extracellular signal-regulated kinases 1 and 2; eNOS, endothelial nitric oxide synthase; Papp, apparent permeability coefficient; CNS, central nervous system; HBMECs, human brain microvascular endothelial cells; OGD, oxygen-glucose deprivation.

* Corresponding author at: Department of Neuroscience, University of Florida, McKnight Brain Institute, 1149 SW Newell Drive, Gainesville, FL 32610, USA.
E-mail addresses: ecandelario@ufl.edu, candelariojalil@yahoo.com (E. Candelario-Jalil).

http://dx.doi.org/10.1016/j.peptides.2016.03.009
0196-9781/

(VEGFR2)/Akt- and VEGFR2/ERK1/2-mediated endothelial nitric oxide synthase (eNOS) activation signaling pathways [28]. Taken together, there is substantial evidence indicating that adropin plays an important role in the regulation of endothelial dysfunction. However, little is known of the effects of adropin on brain endothelial cells and whether this peptide can modulate brain endothelial cell permeability in ischemic conditions.

In this study, we hypothesized that adropin attenuates paracellular permeability of brain endothelial cell monolayers subjected to hypoxia/low glucose (HLG) conditions. We investigated the effects of synthetic adropin$^{34–76}$ on endothelial cell barrier permeability induced by HLG and explored molecular mechanisms that may contribute to its protective effects on endothelial cell permeability. We utilized an *in vitro* BBB model composed of rat brain microvascular endothelial cells (RBE4) grown in Transwell inserts in the presence of astrocyte-conditioned media. We found that adropin$^{34–76}$ significantly reduces endothelial permeability by decreasing Rho-associated kinase (ROCK) activation and myosin light chain 2 (MLC2) phosphorylation, which are key molecular events affecting cytoskeletal structure, cell contractility, and endothelial permeability.

2. Materials and methods

2.1. Cell culture

The rat astrocyte cell line (CTX-TNA2) was obtained from the American Type Culture Collection (Cat. No. CRL-2006; ATCC, Manassas, VA), which was originally established from primary cultures of type 1 astrocytes from brain frontal cortex tissue of one-day old rats. CTX-TNA2 cells (passage 5–20) were maintained in growth media composed of 44% alpha-MEM: 44% Ham's F-10 Nutrient (Cat. Nos. 12571-063 and 11550-043, respectively; Invitrogen, Grand Island, NY) supplemented with 10% heat-inactivated fetal bovine serum (Cat. No. F4135; Sigma-Aldrich, Saint Louis, MO), 1% (100 U/ml) penicillin/(100 μg/ml) streptomycin (Cat. No. 15140-122; Invitrogen, Grand Island, NY), and 1% geneticin (G418, Cat. No. ALX-380-013-G005; 300 μg/ml; Enzo Life Sciences, Farmingdale, NY) at 37 °C in a 5% CO_2 incubator. After reaching confluency, cells were subcultured and conditioned media was collected for use in endothelial cell culture as detailed below.

Rat brain endothelial (RBE4) cells, provided as a gift by Dr. Michael Aschner from the Albert Einstein College of Medicine at Yeshiva University, were grown until confluent on T75 flasks coated with rat tail collagen I at 50 μg/ml (Cat. No. C3867; Sigma-Aldrich, Saint Louis, MO). Cells were initially cultured at 2×10^4 cells/cm^2 for 5 days in astrocyte-conditioned media (ACM) plus freshly prepared 1 ng/ml basic fibroblast growth factor (Cat. No. PHG0264; Invitrogen, Grand Island, NY) and maintained in a humidified 37 °C, 5% CO_2 incubator. Media were replaced every 3 days. The ACM was produced by plating CTX-TNA2 cells on 150-mm dish at 2×10^4 cells/cm^2 and media were harvested every 3 days. The ACM consists of equal parts (1:1, V/V) of fresh astrocyte growth media (alpha-MEM/Ham's F-10 Nutrient containing 10% FBS, 100 U/ml penicillin, 100 μg/ml streptomycin and 300 μg/ml G418) and conditioned astrocyte growth media harvested from the confluent CTX-TNA2 cells. When confluent, RBE4 cells (passages 5 and 15) were trypsinized and harvested.

2.2. In vitro *BBB model using RBE4 cell monolayers*

To establish a BBB model *in vitro*, confluent RBE4 cells grown in T75 flasks for 5 days were trypsinized and seeded at an initial density of 2×10^5 cells/cm^2 on the inner surface of polyethylene terephthalate (PET) cell culture inserts coated with 50 μg/ml of rat tail collagen I (ThinCert™ inserts for 24-well plates, 0.4 μm membrane pore size, Cat. No. 662641; Greiner Bio-One, Monroe, NC). The luminal and abluminal compartments were filled with 200 μl and 800 μl fresh ACM plus EGM-2MV SingleQuot Kit Supplements and Growth Factors (Cat. No. CC-4147, Lonza Walkersville, Inc., Walkersville, MD), respectively. Media were replaced every 3 days. Cells were allowed to grow for 6 days at 37 °C in 5% CO_2 incubator to achieve confluent monolayer and confirmed under a phase contrast microscopy before they were subjected to hypoxia/low glucose (HLG) treatment.

2.3. Hypoxia/low glucose (HLG) conditions

To mimic acute ischemia-like conditions *in vitro*, RBE4 cells grown in the inserts were subjected to HLG treatment. In brief, when the monolayer of cells in 24-well cell culture inserts (for permeability experiments) or 35 mm dishes (for molecular biology experiments) reached confluency after 6 days incubation with ACM plus EGM-2MV SingleQuot Kit Supplements and Growth Factors in a humidified 37 °C, 5% CO_2 incubator, media were replaced with pre-warmed light serum Earle's balanced salt solution (EBSS) containing 1.1 mM D-Glucose plus 5% FBS, where EBSS solution consisted of 117 mM NaCl, 5.5 mM KCl, 1.8 mM $CaCl_2$, 1 mM $MgCl_2$, 20 mM HEPES, 26 mM $NaHCO_3$ and 1 mM NaH_2PO_4. Cultures were then transferred and incubated in a hypoxic atmosphere of 93% N_2, 2% O_2 and 5% CO_2 at 37 °C for 16 h. Once in the chamber, the hypoxic conditions within the chamber were monitored using an electronic oxygen/carbon dioxide analyzer (ProOx Model C21, BioSpherix, Lacona, NY). Control cultures were incubated with normal EBSS containing 5.6 mM D-Glucose plus 5% FBS for 16 h at 37 °C in 95% air and 5% CO_2. After 16 h treatment, cell culture supernatant and cells in 35 mm dishes were collected separately for molecular mechanism analyses, while both luminal and abluminal sides of the inserts were replaced with glucose- and serum-free EBSS. For the paracellular permeability measurements, FITC-dextran was added to the upper chamber of the inserts as described below.

To study the effects of adropin on HLG-induced increase in endothelial permeability, cells were treated with different concentrations (1–100 ng/ml) of adropin$^{34–76}$ (Cat. No. 032-35, Phoenix Pharmaceuticals, Inc., Burlingame, CA) 1 h before and during HLG exposure. To rule out that changes in endothelial permeability in each treatment condition were not due to changes in cell viability, a cytotoxicity/viability assay was performed utilizing the calcein AM fluorescence kit following the manufacturer's protocol (Cat. No. C3099, Molecular Probes, Grand Island, NY).

2.4. Measurement of endothelial monolayer permeability

After exposure to HLG conditions for 16 h, media in both luminal and abluminal sides of the inserts were replaced with EBSS solution. Paracellular permeability was measured by adding 1 mg/ml of fluorescein isothiocyanate (FITC)-conjugated dextran (MW = 40,000 Da; Cat. No. FD40S; Sigma-Aldrich, Saint Louis, MO) to the upper chamber of the insert. After 15 min incubation, FITC-dextran in the lower compartment was detected at excitation/emission wavelengths of 485 and 528 nm, respectively, using a fluorescent multi-mode microplate reader (Biotek, Winooski, VT). A standard curve of different concentrations of the tracer (10–250 ng/ml) was utilized to determine the concentration of FITC-dextran in the lower compartment. The paracellular permeability was then assessed by calculating the apparent permeability coefficient (Papp) as reported [27]. Papp (in centimeters per second) = $dQ/(dt \times A \times Co)$, where dQ is the amount of FITC-dextran getting into the abluminal compartment, dt is the FITC-dextran incubation time (in s), A is the luminal surface area of insert (in

square centimeters), and Co is the initial concentration of FITC-dextran in the luminal insert chamber (in nanograms per cubic centimeter). In each independent experiment, all permeability measurements were performed in triplicate for each treatment condition.

2.5. RNA extraction and real-time PCR

Total RNA was extracted using the PureZOL™ RNA isolation kit (Cat. No. 738-6830; Bio-Rad, Hercules, CA) according to the manufacturer's protocol. The quality and the concentration of the isolated RNA were measured by a Take3 Micro-Volume Plate and Gen5 Data Analysis Software (Biotek Instruments, Winooski, VT). Total RNA was reverse transcribed to cDNA using iScript Reverse Transcription Supermix (Cat. No. 170-8841; Bio-Rad, Hercules, CA) and 1 μg of total RNA in a total volume of 20 μl according to the manufacturer's protocol (Bio-Rad). cDNA synthesis was performed at 25 °C for 5 min, then the reaction was incubated at 42 °C for 30 min followed by 85 °C for 5 min.

Quantitative real-time PCR was performed on a CFX96 Touch Real-Time PCR Detection System (Bio-Rad, Hercules, CA) with 20 ng of cDNA in a total volume of 10 μl using Sso Advanced Universal SYBR Green Supermix (Cat. No. 172-5272; Bio-Rad) according to the manufacturer's protocol. The primer sequences used for amplification of *Enho* were: sense, 5′-GCTCAACTCAGGCTCAGGAC-3′; and antisense, 5′-CGACTTTCCAAGGAGGCTGT-3′ and were normalized to the housekeeping gene *Ywhaz*: sense, 5′-GAAGAGTCGTACAAAGACAGCA-3′; and antisense, 5′- GCTTCTGCTTCGTCTCCTTG-3′. PCR was performed with 40 cycles of initial polymerase activation/DNA denaturation step at 95 °C for 30 s, denaturation at 95 °C for 5 s and annealing at 60 °C for 30 s. Primer specificity was confirmed with a melt curve analysis beginning at 65 °C with increasing increments of 0.5 °C/cycle. PCR reactions were run in triplicate and cycle threshold (Ct) values were normalized to *Ywhaz* expression for each sample. Results are presented as normalized expression relative to RBE4 cells exposed to normoxic conditions.

2.6. Immunoblotting analysis

Cells were harvested in radioimmunoprecipitation (RIPA) buffer consisting of 50 mM Tris-HCl (pH 7.4), 150 mM NaCl, 5 mM EDTA, 1% NP-40, 1% Sodium deoxycholate and 1% SDS plus HALT Protease and Phosphatase Inhibitor Cocktails (Cat. Nos. 78430 and 78428, respectively; Thermo Fisher Scientific, Rockford, IL) and sonicated on ice at 40% amplitude for 10 s on/off for three cycles with a Vibra-Cell sonicator (Model # VCX130PB; Sonics & Materials, Inc., Newton, CT). After 30 min of incubation on ice, the lysates were centrifuged at 14,000*g* for 15 min at 4 °C and supernatants stored at −80 °C until analysis. Thirty micrograms of protein per sample were electrophoresed on a 4–20% SDS-polyacrylamide gel and then transferred onto polyvinylidene fluoride (PVDF) membranes. Membranes were blocked for 1 h at room temperature with 5% non-fat milk in Tris-buffered saline (TBS) before overnight incubation at 4 °C with antibodies against HIF-1α (10006421, 1:500; Cayman Chemical, Ann Arbor, MI), ZO-1 (61–7300, 1:500; Invitrogen, Grand Island, NY), occludin (71–1500, 1:1000; Invitrogen, Grand Island, NY), VE-cadherin (MA5-17050, 1:10,000; Thermo Fisher Scientific Pierce, Rockford, IL), phospho-MLC2 (Ser19) (3671, 1:1000; Cell Signaling Technology, Danvers, MA) and β-actin (A1978, 1:10,000; Sigma-Aldrich, Saint Louis, MO). Membranes were then washed 3 times in TBST and incubated for 1 h with goat anti-rabbit IRDye 800CW (1:30,000; Li-Cor, Lincoln, NE, USA) or donkey anti-mouse IRDye 680LT (1:40,000; Li-Cor) secondary antibodies. β-actin was used as the loading control in whole cell lysate analysis. Immunoreactive bands were visualized and densitometrically analyzed using Odyssey infrared scanner and Image Studio 2.0 software (Li-Cor).

2.7. Adropin ELISA assay

Adropin content in cell culture supernatant was assessed using an ELISA kit (Cat. No. EK-032-35, Phoenix Pharmaceuticals, Inc., Burlingame, CA) according to the manufacturer's protocol. Briefly, aliquots of 200 μl of cell culture supernatants were added to the appropriate microtiter wells provided in the kit. Then, 25 μl of adropin primary antibody and 25 μl of biotinylated adropin peptide were added to each well except the blank wells. The plate was then incubated at room temperature for 2 h. After aspirating and washing 4 times with assay buffer, 100 μl/well of streptavidin-horseradish peroxidase solution was added. Immunoplates were resealed and incubated for 1 h at room temperature. After washing, 100 μl of TMB substrate solution was added to each well and incubated for 1 h at room temperature in the dark before adding 100 μl of 2 N HCl to stop the reaction. Sample absorbance at 450 nm was measured immediately with a Synergy™ HT Multi-Mode Plate Reader (Biotek Instruments, Winooski, VT). A standard curve was constructed (0.01–100 ng/ml) and the concentrations of unknown samples were determined from the standard curve.

2.8. VEGF ELISA assay

VEGF level in cell lysates was measured using a commercially available ELISA kit (Cat. No. ELR-VEGF-CL, RayBiotech, Inc., Norcross, GA). The experiments were performed following the manufacturer's protocol using 1 μg of total protein from cell lysate prepared with RIPA buffer as previously described. Each sample was assayed in duplicate and VEGF concentration in samples was determined based on a standard curve and expressed in picogram per microgram of protein.

2.9. Rho-associated kinase (ROCK) activity assay

ROCK activity in cell lysate was assessed using an ELISA kit (Cat. No. STA-416, Cell Biolabs, Inc., San Diego, CA). In brief, cells were collected in lysis buffer consisting of 50 mM Tris-HCl (pH 7.5), 150 mM NaCl, 1 mM EDTA, 1 mM EGTA, 1 mM 2-glycerophosphate, 1% NP-40, 1% Sodium Orthovanadate and HALT Protease Inhibitor Cocktail (Cat. No. 78430; Thermo Fisher Scientific, Rockford, IL) and sonicated 3 times (10 s/time) followed by 30 min incubation on ice. After incubation, the lysates were centrifuged at 14,000*g* for 15 min at 4 °C and supernatants were saved and assayed for protein concentration. ROCK activity was assessed using 50 μg per sample according to the manufacturer's protocol by quantifying the specific phosphorylation level of myosin phosphatase target subunit 1 (MYPT1) at Thr696. Samples were run in duplicate and the OD values read at 450 nm were analyzed.

2.10. Statistical analysis

All values were expressed as mean ± SEM. Comparisons between two groups were statistically evaluated by unpaired Student's *t*-test. To compare data from more than two groups, statistical analysis was performed by one-way ANOVA followed by Tukey test. A value of $P < 0.05$ was considered statistically significant.

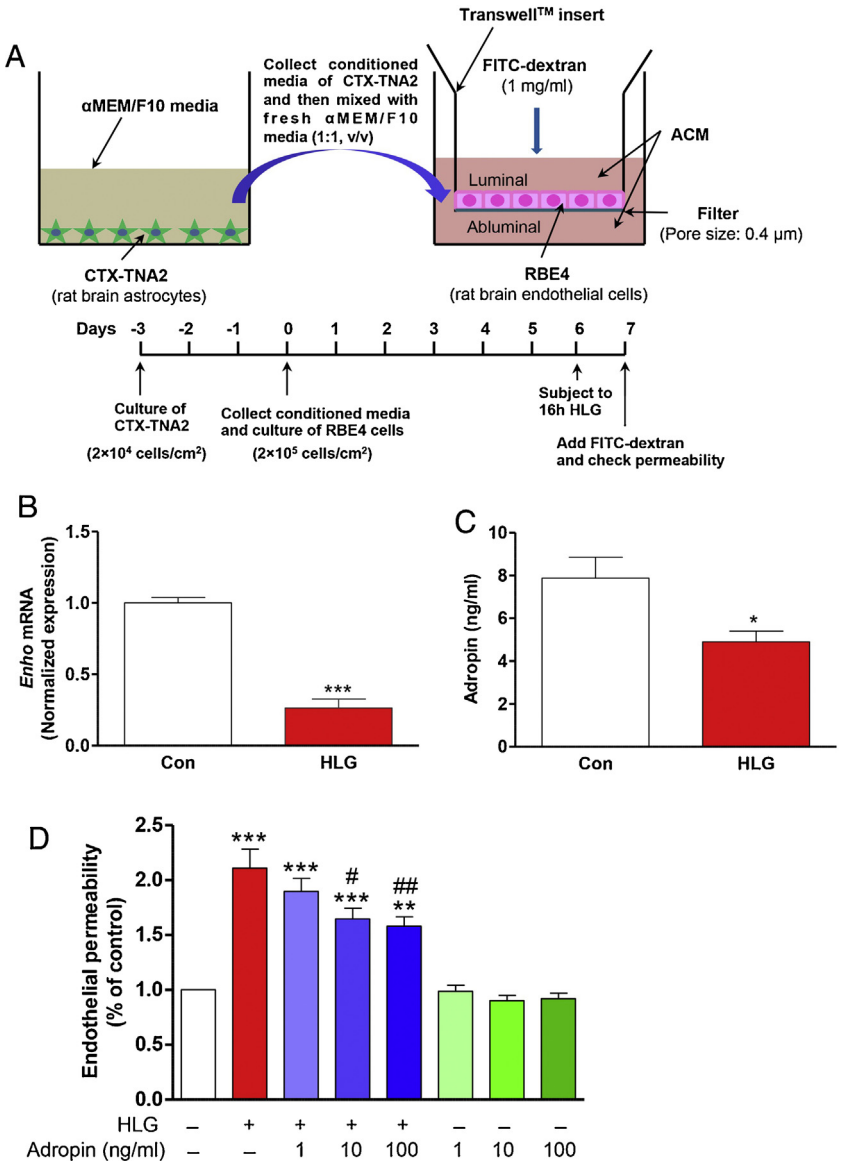

Fig. 1. Role of adropin in the endothelial barrier disruption induced by hypoxia/low glucose (HLG) in RBE4 cells. (A) Schematic drawing of the in vitro blood-brain barrier model (RBE4 cell monolayer grown on an insert in the presence of astrocyte-conditioned media). (B) HLG significantly decreases *Enho* mRNA expression. Data are mean ± SEM of 3 independent experiments performed in triplicate, $^{***}P < 0.001$ *versus* control group. (C) Adropin protein level. ELISA measurements depict reduced adropin content in cell culture media in response to HLG. Data are mean ± SEM, $^{*}P < 0.05$ *versus* control group, n = 7. (D) Adropin concentration-dependently attenuates HLG-induced endothelial permeability. Endothelial monolayer permeability was assessed by calculating the transfer rate of FITC-dextran (40 kDa) from the luminal to the abluminal compartment and was expressed as % of control (normoxic) apparent permeability coefficient (Papp). Exposure of RBE4 cells monolayer to HLG for 16 h significantly increased its permeability to FITC-dextran. Pretreatment of RBE4 cells with adropin$^{34-76}$ (1, 10 and 100 ng/ml) for 60 min before subjecting them to HLG significantly reduced HLG-induced paracellular permeability in a dose dependent manner, while adropin$^{34-76}$ alone had no effect on endothelial permeability. Data are mean ± SEM of 5 independent experiments performed in triplicate, $^{**}P < 0.01$, $^{***}P < 0.001$ *versus* control group and $^{\#}P < 0.05$, $^{\#\#}P < 0.01$ compared to HLG.

3. Results

3.1. *HLG induces a significant downregulation of* Enho *mRNA expression and a marked decrease in adropin production by RBE4 cells*

To study the effects of adropin on brain endothelial permeability, we first established an *in vitro* BBB model composed of rat brain microvascular endothelial cells (RBE4) cultured in astrocyte-conditioned media and subjected to 16 h hypoxia/low glucose (HLG, 2% O_2, 1.1 mM D-glucose) to mimic the changes during an ischemic stroke (Fig. 1A). Exposure to HLG conditions resulted in a dramatic increase in paracellular permeability measured by the transfer rate of FITC-dextran from the luminal compartment to the abluminal compartment (Papp, apparent permeability coefficient; Fig. 1D).

To determine whether the HLG-induced increase in endothelial permeability was due to endothelial cell death, we quantified cell viability with calcein AM. We observed no significant difference in calcein fluorescence intensity between the control and HLG groups (data not shown), ruling out the possibility that HLG-induced endothelial barrier disruption is due to changes in endothelial cell viability.

Adropin is abundantly expressed in liver and brain [24,42], and has beneficial effects on endothelial function in the periphery [28]. However, it remains unknown if brain endothelial cells produce adropin and whether this peptide modulates brain endothelial cell permeability. Exposure of RBE4 cells to HLG conditions dramati-

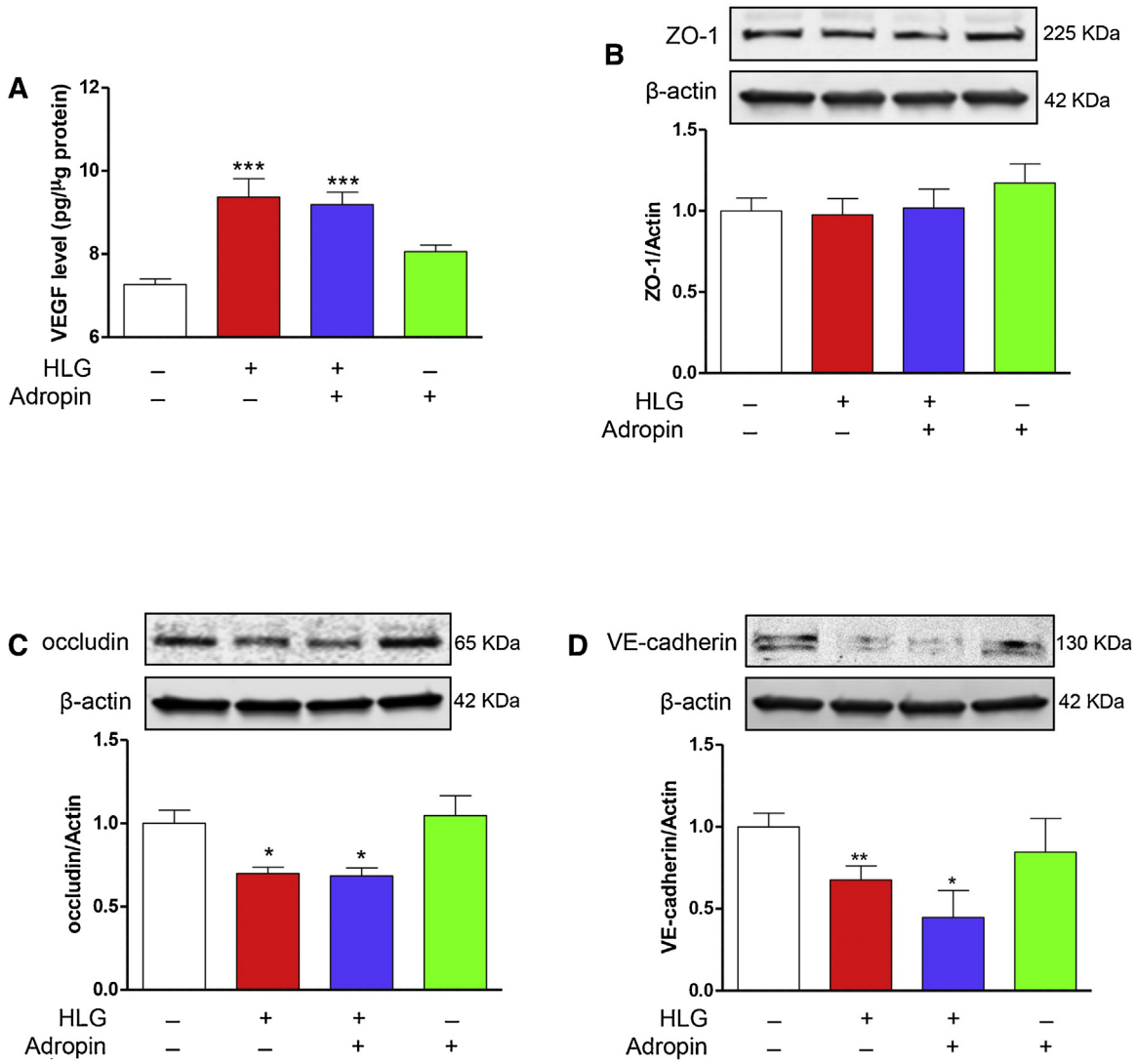

Fig. 2. Effect of Adropin on VEGF, ZO-1, occludin and VE-cadherin protein levels after HLG treatment in RBE4 cells. (A) VEGF protein level in RBE4 cells was measured by ELISA. Exposure of cells to HLG for 16 h significantly increased VEGF protein level; adropin$^{34–76}$ failed to reduce HLG-induced VEGF production. Data are mean ± SEM, $^{***}P < 0.001$ *versus* control group, n = 8. ZO-1 (B), occludin (C) and VE-cadherin (D) in total cell lysate were detected by Western blot and densitometric data are presented as percentage of control group. HLG caused degradation of occludin and VE-cadherin, but did not affect ZO-1. Pretreatment of RBE4 cells with adropin$^{34–76}$ (10 ng/ml) had no effect on ZO-1, occludin, and VE-cadherin in response to HLG conditions. Data are mean ± SEM, $^{*}P < 0.05$, $^{**}P < 0.01$ *versus* control group, n = 3–6/group.

cally reduced *Enho* mRNA expression compared to the normoxic controls, as quantified using real-time PCR (Fig. 1B). In line with the PCR results, we found a significant reduction in adropin levels in the RBE4 cell media when exposed to HLG compared with controls, as assessed by a commercially available ELISA assay kit (Fig. 1C). These data suggest the possibility that adropin might modulate endothelial barrier integrity during ischemia-like conditions.

3.2. Adropin concentration-dependently attenuates the increase in paracellular permeability induced by HLG in RBE4 cells

We next evaluated whether adropin could affect endothelial monolayer permeability in RBE4 cells exposed to ischemia-like conditions. As shown in Fig. 1D, pretreatment of RBE4 cells with synthetic adropin$^{34–76}$ peptide (1, 10 and 100 ng/ml) for 60 min significantly reduced the increase in paracellular permeability to FITC-dextran induced by HLG in a concentration-dependent manner, while treatment of control RBE4 cells with the same concentrations of adropin alone had no effect on basal endothelial permeability. In the following experiments, 10 ng/ml adropin$^{34–76}$ peptide was selected for the molecular mechanism studies.

3.3. HLG causes dramatic endothelial barrier disruption associated with increased VEGF production, and loss of occludin and VE-cadherin in RBE4 cells

To explore the underlying mechanisms contributing to endothelial barrier damage by HLG, we assessed the protein levels of hypoxia inducible factor-1alpha (HIF-1α) and one of its downstream effectors, vascular endothelial growth factor (VEGF). These mediators have been shown to increase BBB damage induced by hypoxia [45] or oxygen and glucose deprivation [7]. As expected, we observed a dramatic increase in HIF-1α protein after exposure of endothelial cells to HLG for 16 h when compared to control conditions (data not shown). Similarly, HLG induced an increase in VEGF production in RBE4 cells quantified with an ELISA (Fig. 2A). Using immunoblotting, we next examined changes in two important tight junction proteins, zonula occludens-1 (ZO-1) and occludin, as well as one of the critical adherens junction proteins, vascular endothe-

lial cadherin (VE-cadherin). There were no changes in ZO-1 protein levels (Fig. 2B), but a significant reduction in occludin and VE-cadherin was observed in HLG compared to control conditions (Fig. 2C and D). These findings suggest that increase in VEGF or loss of junction proteins might contribute to endothelial barrier disruption in the HLG conditions.

3.4. Adropin-mediated reduction in endothelial permeability is not dependent on VEGF

Increased VEGF signaling has been shown to mediate endothelial permeability changes during hypoxia and other stimuli [16,32]. To determine whether changes in VEGF levels were involved in adropin-mediated reduction of endothelial permeability in RBE4 cells exposed to HLG conditions, VEGF levels in cell lysates were quantified with an ELISA. As shown in Fig. 2A, HLG significantly increased VEGF protein level with respect to the control condition, adropin (10 ng/ml) had no effect on either basal (normoxic conditions) or HLG-induced VEGF production.

3.5. Adropin has no effect on HLG-induced changes in tight junction or adherens junction proteins

Since tight junction and adherens junction proteins are important in maintaining the low paracellular permeability of the brain microvasculature, we investigated the effects of adropin on HLG-mediated loss of adherens and tight junction protein complexes. As shown in Fig. 2B, tight junction protein ZO-1 was unchanged after HLG treatment, and there was no effect with adropin treatment. However, occludin was significantly reduced by HLG, and adropin treatment had no effect on HLG-mediated loss of this tight junction protein (Fig. 2C). Since cellular redistribution of ZO-1 and occludin proteins can alter barrier permeability without changing the overall protein levels, we analyzed potential changes in these two tight junction proteins in cytosol, membrane, and cytoskeletal fractions. We found that HLG decreased cytosolic levels of ZO-1 and increased its levels in the membrane fraction. No alterations in the redistribution of occludin were seen following HLG exposure. Adropin had no effect on the cellular redistribution of ZO-1 in this model (data not shown). In parallel, a significant reduction of VE-cadherin, one of the critical adherens junction proteins, was also observed after HLG treatment, but pretreatment of RBE4 cells with adropin did not prevent HLG-induced loss of VE-cadherin (Fig. 2D). These findings indicate that preservation of key proteins composing the adherens and tight junction complexes does not underlie the protective effects of adropin on endothelial barrier function during HLG conditions.

3.6. Adropin significantly reduces the upregulation of MLC2 phosphorylation and ROCK activity in cells exposed to ischemia-like conditions

In continued efforts to explore the underlying mechanism of adropin-mediated reduction in paracellular permeability induced by HLG, we examined the role of endothelial cell contraction in regulation of endothelial permeability. It is well documented that activation of Rho/ROCK with the resulting increase in MLC2 phosphorylation plays an important role in actomyosin contractility and weakening of cell–cell interactions between adjacent endothelial cells, which leads to increase in paracellular permeability [33,34,36]. Immunoblotting results shown in Fig. 3A indicate that HLG increased by 2.7-fold the phosphorylation of MLC2 at the Ser19 site compared to the control group and adropin treatment significantly reduced MLC2 phosphorylation induced by HLG. Next, we measured the activation of ROCK, which is a critical upstream effector of myosin light chain phosphatase (MLCP) inhibition resulting

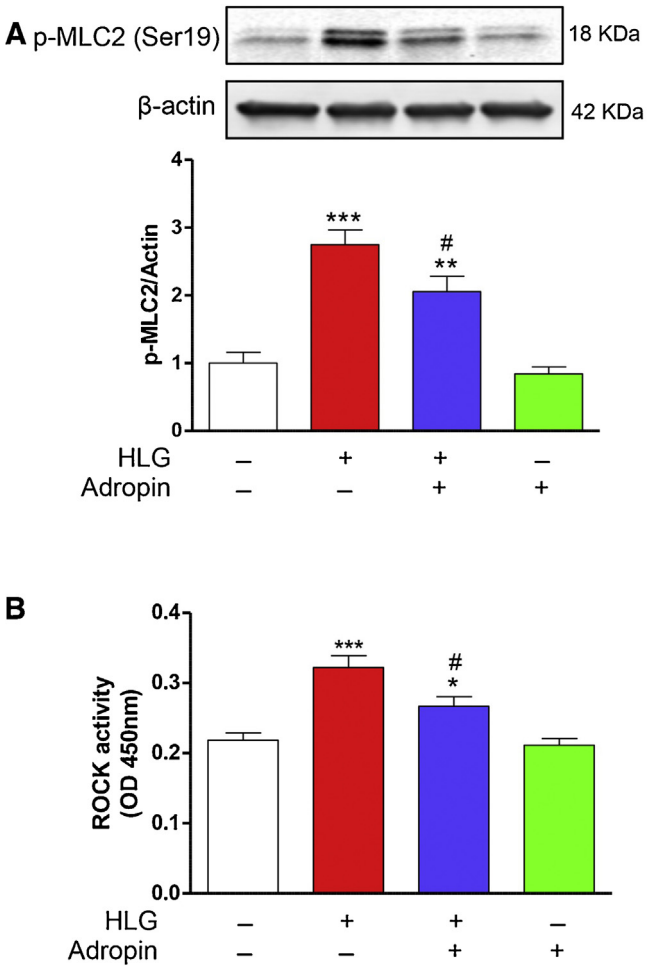

Fig. 3. Effect of Adropin on MLC2 phosphorylation and ROCK activity after HLG treatment in RBE4 cells. (A) Phosphorylation of MLC2 (Ser19) in total cell lysate was detected by Western blot and densitometric data are presented as percentage of control group. HLG resulted in a marked increase in myosin light chain (MLC2) phosphorylation at Ser19 site, and adropin$^{34-76}$ (10 ng/ml) significantly reduced HLG-induced MLC2 phosphorylation in RBE4 cells. Data are mean ± SEM, $^{**}P < 0.01$, $^{***}P < 0.001$ *versus* control group and $^{\#}P < 0.05$ compared to HLG, n = 6. (B) ROCK activity in RBE4 cells was measured by ELISA. Exposure of cells to HLG for 16 h increased ROCK activity, and adropin$^{34-76}$ (10 ng/ml) significantly reduced its activity induced by HLG. Data are mean ± SEM, $^{*}P < 0.05$, $^{***}P < 0.001$ *versus* control group and $^{\#}P < 0.05$ compared to HLG, n = 6.

in an increase in MLC2 phosphorylation [33,34]. HLG significantly increased ROCK activity in RBE4 cells and a significant reduction in ROCK activation was found in endothelial cells treated with adropin compared to HLG-treated cells, as shown in Fig. 3B. Taken together, these data suggest that inhibition of the ROCK-MLC2 signaling pathway by adropin may play an important role in its protective effects against HLG-induced endothelial cell barrier damage.

4. Discussion

In the current study, we employed an in vitro BBB model of RBE4 cells cultured in astrocyte-conditioned media to investigate the effects of adropin on endothelial cell permeability during ischemia-like conditions and explore molecular mechanisms underlying the effects of adropin on brain endothelial cell function. We hypothesized that adropin would reduce endothelial cell permeability during ischemia-like conditions. We found that HLG resulted in a significant increase of endothelial permeability in RBE4 cells, associated with downregulation of *Enho* expression and adropin protein level. Pretreatment of RBE4 cells with exogenous adropin peptide

significantly reduced endothelial cell permeability induced by HLG in a concentration-dependent manner. Molecular studies indicated that HLG-induced endothelial cell permeability was associated with a dramatic upregulation of VEGF, and the loss of junction proteins occludin and VE-cadherin, but the protective effect of adropin on endothelial barrier function against HLG injury was not mediated through protection to junction proteins or through reduced levels of VEGF. We found that HLG dramatically increased MLC2 phosphorylation in RBE4 cells, which was significantly reduced by adropin pretreatment. Further findings indicated that HLG significantly increased ROCK activity, a critical upstream effector of MLC2 phosphorylation, and that adropin pretreatment attenuated that effect. Taken together, these data suggest that pretreatment with adropin can reduce RBE4 cell permeability after HLG insult by inhibition of the ROCK-MLC2 signaling pathway.

Accumulating evidence indicates that BBB breakdown accompanies ischemic stroke and is exacerbated by recombinant tissue plasminogen activator (tPA), the only FDA-approved thrombolytic therapy for acute ischemic stroke [22,23]. Damage to the BBB negatively impacts stroke outcomes. Thus, development of novel therapeutic strategies aimed at maintaining BBB integrity could be promising in attenuating brain injury after stroke.

Endothelial cells are the core component of the BBB, supported by astrocytes, pericytes, perivascular microglia, neurons and the basal lamina to form a fully functional neurovascular unit [21]. Data from a considerable number of studies indicate that astrocytes are implicated in the induction of a BBB phenotype in *in vitro* cell culture systems [9,38]. In agreement with these reports, our *in vitro* BBB model (culture of RBE4 cells with astrocyte-conditioned media) also exhibits typical barrier function with lower permeability to FITC-dextran compared to RBE4 cells with normal growth media alone, suggesting that astrocyte-derived factors play an important role in the induction of BBB properties.

When blood flow to the brain is suddenly blocked by a thrombus or embolism, brain tissue is deprived of oxygen and glucose, which subsequently triggers the stroke injury cascade associated with BBB damage. To mimic microvascular injury following cerebral ischemia, we subjected a confluent RBE4 cell monolayer to HLG (2% O_2, 1.1 mM D-glucose) for 16 h. This resulted in increased endothelial cell permeability, which was associated with upregulation of hypoxia-sensitive transcription factor HIF-1α and its downstream-regulated protein VEGF. Importantly, degradation of the tight junction protein occludin and the adherens junction protein VE-cadherin was also observed in our model. These findings suggest that the HLG-mediated RBE4 cell monolayer permeability increase may be through the accumulation of upstream effectors of HIF-1α and VEGF, thus ultimately resulting in the degradation of key structural components that seal the gaps between adjacent endothelial cells. A previous study showed that a potent inhibitor of HIF-1α, YC-1, significantly protected against hypoxia or ischemia-induced injury *in vitro* and *in vivo* by inhibiting HIF-1α accumulation, VEGF production and preventing tight junction protein ZO-1 degradation [45]. Furthermore, it has been shown that VEGF promotes the internalization of VE-cadherin, which results in endothelial barrier disruption by altering the composition of tight junction complexes [19,37]. This mechanism could explain, at least in part, the increased paracellular permeability seen in our model following exposure of RBE4 cells to HLG conditions.

In the light of previous evidence showing that adropin enhances endothelial function in the periphery, we investigated the effects of adropin on an *in vitro* BBB model exposed to HLG to mimic ischemic conditions. Although a majority of studies report that adropin plays a critical role in the regulation of metabolic homeostasis and insulin sensitivity [8,17,18,24,35], emerging evidence indicates that low serum adropin level is associated with cardiovascular diseases and endothelial dysfunction in patients [10,43,46,47,49]. Furthermore, a recent *in vitro* study using human umbilical vein and coronary artery endothelial cells found that adropin-treated endothelial cells exhibited reduced endothelial permeability [28], supporting the possibility that adropin might also play an important role in the regulation of brain endothelial barrier function. To test this hypothesis, we examined whether the adropin gene *Enho* and adropin protein levels were changed in rat brain endothelial cells exposed to HLG treatment. Notably, both *Enho* mRNA and adropin protein levels are dramatically down-regulated in RBE4 cells subjected to 16 h HLG treatment. In view of these findings, we determined whether treatment with exogenous adropin could attenuate endothelial cell permeability induced by HLG in RBE4 cells. We pretreated RBE4 cells for one hour with adropin$^{34–76}$ peptide before they were subjected to HLG. Adropin$^{34–76}$ decreased HLG-induced endothelial cell permeability in a concentration-dependent manner, while treatment of RBE4 cells with adropin$^{34–76}$ alone had no effect on endothelial permeability. Taken together, these data strongly suggest that adropin plays a role in the protection of endothelial cell barrier function during ischemic conditions.

To elucidate the mechanism by which adropin attenuates HLG-induced increase in endothelial permeability, we examined levels of VEGF in RBE4 cells after HLG with or without adropin$^{34–76}$ pretreatment since it has been documented that VEGF promotes BBB disruption in brain injury [4,32,48]. HLG dramatically increased VEGF levels compared to control cells, but adropin did not reduce VEGF levels. These findings suggest that VEGF signaling might play an important role in HLG-induced endothelial barrier disruption in RBE4 cells. However, based on our results, the protective effects of adropin do not seem to depend on changes in VEGF levels during HLG conditions.

We next examined the effects of adropin on HLG-induced alteration of tight junctions and adherens junctions since they are important in the maintenance of BBB function [1]. Occludin is one of critical transmembrane tight junction proteins that interact with accessory proteins to seal the gap between cells [29], and the cytoplasmic scaffolding protein ZO-1 is the major cross-linker anchoring the tight junction strand proteins to the actin-based cytoskeleton, which is required for the stabilization of tight junctions [14]. VE-cadherin is the primary component of adherens junctions, which also mediates cell–cell adhesion to maintain vascular endothelial barrier integrity [40]. In our study, we observed decreased levels of occludin and VE-cadherin, but no change in ZO-1 after HLG treatment. These findings are consistent with previous reports showing that disassembly or loss of specific tight junction or adherens junction proteins is associated with the opening of BBB [5,6,11,15,26]. However, pretreatment with adropin did not recover levels of occludin and VE-cadherin compared to HLG alone, indicating that the protective effects of adropin on HLG-induced endothelial barrier failure are not mediated by changes in junction protein expression.

In addition to the role of junction proteins in the regulation of BBB disruption, it has been well documented that actomyosin-based cell contractility significantly contributes to the increase of endothelial cell layer permeability [31,33,44]. The Rho signaling pathway is being increasingly recognized as an important determinant of cell motility and cytoskeletal structure [30]. The phosphorylation of MLC2 at Ser19 is an indicator of the activation of Rho signaling because it is well known that the Ser19 of MLC2 is specifically phosphorylated *via* ROCK [30], and that the resulting MLC2 phosphorylation plays a pivotal role in cell contraction through its interaction with actin–myosin [3]. It was reported that thrombin increased endothelial cell permeability in human endothelial cells by increasing actomyosin contractility and MLC2 phosphorylation *via* Rho and its target ROCK [13]. More recently, it has been shown that oxygen-glucose deprivation (OGD) significantly increased ROCK protein expression and activity in human

brain microvascular endothelial cells (HBMECs), which was associated with breakdown of the endothelial cell barrier [2]. Importantly, OGD enhanced both total and Thr18/Ser19 MLC2 phosphorylation in HBMEC, which was associated with a dramatic increase in Rho/ROCK activation. Blockade of RhoA with a specific antibody or pharmacological inhibition of ROCK significantly reduced endothelial cell barrier permeability and MLC2 phosphorylation [2]. Also, there is evidence that ROCK can directly phosphorylate MLC2 *in vitro* acting as a MLC kinase, and that the primary phosphorylation site of MLC2 by ROCK is Ser19 [3]. Our results obtained in HLG-induced endothelial cells seem to support this notion. HLG dramatically increased MLC2 phosphorylation at Ser19 and ROCK activity, and these effects are significantly reduced by pretreatment with adropin. Taken together, these findings suggest that modulation of ROCK-MLC2 signaling pathway by adropin may play an important role in its beneficial effects on endothelial barrier integrity during ischemia-like conditions.

In summary, we report for the first time that adropin is expressed in RBE4 cells and both *Enho* mRNA and protein levels are downregulated after HLG treatment. We found that pretreatment with adropin peptide attenuates HLG-induced endothelial barrier damage in a concentration-dependent manner. We also report a novel mechanism through which adropin-mediated reduction in brain endothelial cell barrier permeability under HLG condition may occur *via* inhibition of the ROCK-MLC2 pathway, resulting in attenuation of endothelial cell contractile function. Findings in this study indicate adropin as a potential target to reduce endothelial cell barrier permeability, which could be promising in new efforts to reduce BBB breakdown in ischemic stroke.

Conflict of interest disclosure

The authors declare that they have no competing interests.

Authors' contributions

CY and ECJ conceived and designed research; ECJ led the project; CY, KMD and KEH performed experiments; CY and ECJ performed data analysis and wrote the paper. All authors read and approved the final manuscript.

Acknowledgement

This research was supported by the Brain and Spinal Cord Injury Research Trust Fund, McKnight Brain Institute, University of Florida.

References

[1] N.J. Abbott, A.A. Patabendige, D.E. Dolman, S.R. Yusof, D.J. Begley, Structure and function of the blood-brain barrier, Neurobiol. Dis. 37 (2010) 13–25.
[2] C. Allen, K. Srivastava, U. Bayraktutan, Small GTPase RhoA and its effector rho kinase mediate oxygen glucose deprivation-evoked in vitro cerebral barrier dysfunction, Stroke 41 (2010) 2056–2063.
[3] M. Amano, M. Ito, K. Kimura, Y. Fukata, K. Chihara, T. Nakano, et al., Phosphorylation and activation of myosin by Rho-associated kinase (Rho-kinase), J. Biol. Chem. 271 (1996) 20246–20249.
[4] A.T. Argaw, L. Asp, J. Zhang, K. Navrazhina, T. Pham, J.N. Mariani, et al., Astrocyte-derived VEGF-A drives blood-brain barrier disruption in CNS inflammatory disease, J. Clin. Invest. 122 (2012) 2454–2468.
[5] A.T. Bauer, H.F. Burgers, T. Rabie, H.H. Marti, Matrix metalloproteinase-9 mediates hypoxia-induced vascular leakage in the brain via tight junction rearrangement, J. Cereb. Blood Flow Metab. 30 (2010) 837–848.
[6] S.J. Bolton, D.C. Anthony, V.H. Perry, Loss of the tight junction proteins occludin and zonula occludens-1 from cerebral vascular endothelium during neutrophil-induced blood-brain barrier breakdown in vivo, Neuroscience 86 (1998) 1245–1257.
[7] A. Bulbarelli, E. Lonati, A. Brambilla, A. Orlando, E. Cazzaniga, F. Piazza, et al., Abeta42 production in brain capillary endothelial cells after oxygen and glucose deprivation, Mol. Cell. Neurosci. 49 (2012) 415–422.
[8] A.A. Butler, C.S. Tam, K.L. Stanhope, B.M. Wolfe, M.R. Ali, M. O'Keeffe, et al., Low circulating adropin concentrations with obesity and aging correlate with risk factors for metabolic disease and increase after gastric bypass surgery in humans, J. Clin. Endocrinol. Metab. 97 (2012) 3783–3791.
[9] C.A. Cantrill, R.A. Skinner, N.J. Rothwell, J.I. Penny, An immortalised astrocyte cell line maintains the in vivo phenotype of a primary porcine in vitro blood-brain barrier model, Brain Res. 1479 (2012) 17–30.
[10] A. Celik, M. Balin, M.A. Kobat, K. Erdem, A. Baydas, M. Bulut, et al., Deficiency of a new protein associated with cardiac syndrome X; called adropin, Cardiovasc. Ther. 31 (2013) 174–178.
[11] E. Dejana, F. Orsenigo, M.G. Lampugnani, The role of adherens junctions and VE-cadherin in the control of vascular permeability, J. Cell Sci. 121 (2008) 2115–2122.
[12] J.P. Desilles, A. Rouchaud, J. Labreuche, E. Meseguer, J.P. Laissy, J.M. Serfaty, et al., Blood-brain barrier disruption is associated with increased mortality after endovascular therapy, Neurology 80 (2013) 844–851.
[13] M. Essler, M. Amano, H.J. Kruse, K. Kaibuchi, P.C. Weber, M. Aepfelbacher, Thrombin inactivates myosin light chain phosphatase via Rho and its target Rho kinase in human endothelial cells, J. Biol. Chem. 273 (1998) 21867–21874.
[14] A.S. Fanning, B.J. Jameson, L.A. Jesaitis, J.M. Anderson, The tight junction protein ZO-1 establishes a link between the transmembrane protein occludin and the actin cytoskeleton, J. Biol. Chem. 273 (1998) 29745–29753.
[15] S. Feng, J. Cen, Y. Huang, H. Shen, L. Yao, Y. Wang, et al., Matrix metalloproteinase-2 and -9 secreted by leukemic cells increase the permeability of blood-brain barrier by disrupting tight junction proteins, PLoS One 6 (2011) e20599.
[16] S. Fischer, M. Clauss, M. Wiesnet, D. Renz, W. Schaper, G.F. Karliczek, Hypoxia induces permeability in brain microvessel endothelial cells via VEGF and NO, Am. J. Physiol. 276 (1999) C812–20.
[17] K. Ganesh Kumar, J. Zhang, S. Gao, J. Rossi, O.P. McGuinness, H.H. Halem, et al., Adropin deficiency is associated with increased adiposity and insulin resistance, Obesity (Silver Spring) 20 (2012) 1394–1402.
[18] S. Gao, R.P. McMillan, Q. Zhu, G.D. Lopaschuk, M.W. Hulver, A.A. Butler, Therapeutic effects of adropin on glucose tolerance and substrate utilization in diet-induced obese mice with insulin resistance, Mol. Metab. 4 (2015) 310–324.
[19] J. Gavard, J.S. Gutkind, VEGF controls endothelial-cell permeability by promoting the beta-arrestin-dependent endocytosis of VE-cadherin, Nat. Cell Biol. 8 (2006) 1223–1234.
[20] D. Gozal, L. Kheirandish-Gozal, R. Bhattacharjee, H. Molero-Ramirez, H.L. Tan, H.P. Bandla, Circulating adropin concentrations in pediatric obstructive sleep apnea: potential relevance to endothelial function, J. Pediatr. 163 (2013) 1122–1126.
[21] B.T. Hawkins, T.P. Davis, The blood-brain barrier/neurovascular unit in health and disease, Pharmacol. Rev. 57 (2005) 173–185.
[22] X. Jin, J. Liu, W. Liu, Early ischemic blood brain barrier damage: a potential indicator for hemorrhagic transformation following tissue plasminogen activator (tPA) thrombolysis, Curr. Neurovasc. Res. 11 (2014) 254–262.
[23] T. Kahles, C. Foerch, M. Sitzer, M. Schroeter, H. Steinmetz, A. Rami, et al., Tissue plasminogen activator mediated blood-brain barrier damage in transient focal cerebral ischemia in rats: relevance of interactions between thrombotic material and thrombolytic agent, Vasc. Pharmacol. 43 (2005) 254–259.
[24] K.G. Kumar, J.L. Trevaskis, D.D. Lam, G.M. Sutton, R.A. Koza, V.N. Chouljenko, et al., Identification of adropin as a secreted factor linking dietary macronutrient intake with energy homeostasis and lipid metabolism, Cell Metab. 8 (2008) 468–481.
[25] L.L. Latour, D.W. Kang, M.A. Ezzeddine, J.A. Chalela, S. Warach, Early blood-brain barrier disruption in human focal brain ischemia, Ann. Neurol. 56 (2004) 468–477.
[26] H.S. Lee, K. Namkoong, D.H. Kim, K.J. Kim, Y.H. Cheong, S.S. Kim, et al., Hydrogen peroxide-induced alterations of tight junction proteins in bovine brain microvascular endothelial cells, Microvasc. Res. 68 (2004) 231–238.
[27] J. Liu, X. Jin, K.J. Liu, W. Liu, Matrix metalloproteinase-2-mediated occludin degradation and caveolin-1-mediated claudin-5 redistribution contribute to blood-brain barrier damage in early ischemic stroke stage, J. Neurosci. 32 (2012) 3044–3057.
[28] F. Lovren, Y. Pan, A. Quan, K.K. Singh, P.C. Shukla, M. Gupta, et al., Adropin is a novel regulator of endothelial function, Circulation 122 (2010) S185–92.
[29] K.M. McCarthy, I.B. Skare, M.C. Stankewich, M. Furuse, S. Tsukita, R.A. Rogers, et al., Occludin is a functional component of the tight junction, J. Cell Sci. 109 (Pt 9) (1996) 2287–2298.
[30] K. Riento, A.J. Ridley, Rocks multifunctional kinases in cell behaviour, Nat. Rev. Mol. Cell Biol. 4 (2003) 446–456.
[31] H.J. Schnittler, A. Wilke, T. Gress, N. Suttorp, D. Drenckhahn, Role of actin and myosin in the control of paracellular permeability in pig, rat and human vascular endothelium, J. Physiol. 431 (1990) 379–401.
[32] H.J. Schoch, S. Fischer, H.H. Marti, Hypoxia-induced vascular endothelial growth factor expression causes vascular leakage in the brain, Brain 125 (2002) 2549–2557.
[33] Q. Shen, R.R. Rigor, C.D. Pivetti, M.H. Wu, S.Y. Yuan, Myosin light chain kinase in microvascular endothelial barrier function, Cardiovasc. Res. 87 (2010) 272–280.
[34] A.P. Somlyo, A.V. Somlyo, Signal transduction by G-proteins, rho-kinase and protein phosphatase to smooth muscle and non-muscle myosin II, J. Physiol. 522 (Pt 2) (2000) 177–185.

[35] M.P. St-Onge, A. Shechter, J. Shlisky, C.S. Tam, S. Gao, E. Ravussin, et al., Fasting plasma adropin concentrations correlate with fat consumption in human females, Obesity (Silver Spring) 22 (2014) 1056–1063.
[36] J. Sturge, D. Wienke, C.M. Isacke, Endosomes generate localized Rho-ROCK-MLC2-based contractile signals via Endo180 to promote adhesion disassembly, J. Cell Biol. 175 (2006) 337–347.
[37] A. Taddei, C. Giampietro, A. Conti, F. Orsenigo, F. Breviario, V. Pirazzoli, et al., Endothelial adherens junctions control tight junctions by VE-cadherin-mediated upregulation of claudin-5, Nat. Cell Biol. 10 (2008) 923–934.
[38] J.H. Tao-Cheng, Z. Nagy, M.W. Brightman, Tight junctions of brain endothelium in vitro are enhanced by astroglia, J. Neurosci. 7 (1987) 3293–3299.
[39] M. Topuz, A. Celik, T. Aslantas, A.K. Demir, S. Aydin, Plasma adropin levels predict endothelial dysfunction like flow-mediated dilatation in patients with type 2 diabetes mellitus, J. Invest. Med. 61 (2013) 1161–1164.
[40] D. Vestweber, VE-cadherin: the major endothelial adhesion molecule controlling cellular junctions and blood vessel formation, Arterioscler. Thromb. Vasc. Biol. 28 (2008) 223–232.
[41] S. Warach, L.L. Latour, Evidence of reperfusion injury, exacerbated by thrombolytic therapy, in human focal brain ischemia using a novel imaging marker of early blood-brain barrier disruption, Stroke 35 (2004) 2659–2661.
[42] C.M. Wong, Y. Wang, J.T. Lee, Z. Huang, D. Wu, A. Xu, et al., Adropin is a brain membrane-bound protein regulating physical activity via the NB-3/Notch signaling pathway in mice, J. Biol. Chem. 289 (2014) 25976–25986.
[43] L. Wu, J. Fang, L. Chen, Z. Zhao, Y. Luo, C. Lin, et al., Low serum adropin is associated with coronary atherosclerosis in type 2 diabetic and non-diabetic patients, Clin. Chem. Lab. Med. 52 (2014) 751–758.
[44] L. Wu, S.H. Ramirez, A.M. Andrews, W. Leung, K. Itoh, J. Wu, et al., Neuregulin1-beta decreases IL-1beta induced RhoA activation, myosin light chain phosphorylation, and endothelial hyper-permeability, J. Neurochem. 136 (2016) 250–257, http://dx.doi.org/10.1111/jnc.13374/abstract.
[45] W.L. Yeh, D.Y. Lu, C.J. Lin, H.C. Liou, W.M. Fu, Inhibition of hypoxia-induced increase of blood-brain barrier permeability by YC-1 through the antagonism of HIF-1alpha accumulation and VEGF expression, Mol. Pharmacol. 72 (2007) 440–449.
[46] H.Y. Yu, P. Zhao, M.C. Wu, J. Liu, W. Yin, Serum adropin levels are decreased in patients with acute myocardial infarction, Regul. Pept. 190–191 (2014) 46–49.
[47] C. Zhang, L. Zhao, W. Xu, J. Li, B. Wang, X. Gu, et al., Correlation of serum adropin level with coronary artery disease, Zhonghua Yi Xue Za Zhi 94 (2014) 1255–1257.
[48] Z.G. Zhang, L. Zhang, Q. Jiang, R. Zhang, K. Davies, C. Powers, et al., VEGF enhances angiogenesis and promotes blood-brain barrier leakage in the ischemic brain, J. Clin. Invest. 106 (2000) 829–838.
[49] L.P. Zhao, W.T. Xu, L. Wang, T. You, S.P. Chan, X. Zhao, et al., Serum adropin level in patients with stable coronary artery disease, Heart Lung Circ. 24 (2015) 975–979 http://www.ncbi.nlm.nih.gov/pubmed/25912996.